Article

Hydrogen Atom Transfer Reactions of Imido Manganese(V) Corrole: One Reaction with Two Mechanistic Pathways

Michael J. Zdilla, Jennifer L. Dexheimer, and Mahdi M. Abu-Omar

J. Am. Chem. Soc., **2007**, 129 (37), 11505-11511• DOI: 10.1021/ja073027s • Publication Date (Web): 25 August 2007

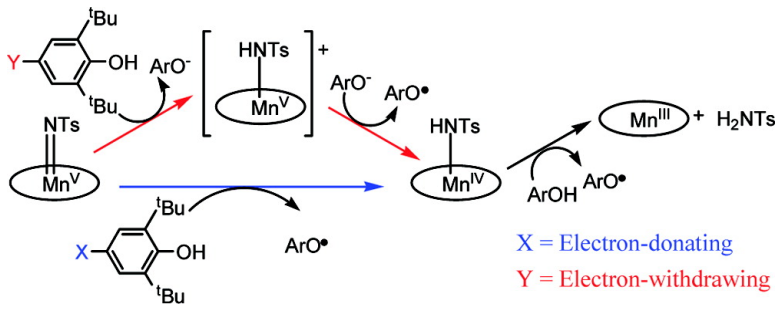

More About This Article

Additional resources and features associated with this article are available within the HTML version:

- Supporting Information
- Links to the 5 articles that cite this article, as of the time of this article download
- Access to high resolution figures
- Links to articles and content related to this article
- Copyright permission to reproduce figures and/or text from this article

View the Full Text HTML

J|A|C|S
ARTICLES
Published on Web 08/25/2007

Hydrogen Atom Transfer Reactions of Imido Manganese(V) Corrole: One Reaction with Two Mechanistic Pathways

Michael J. Zdilla, Jennifer L. Dexheimer, and Mahdi M. Abu-Omar*

Contribution from the Brown Laboratory, Department of Chemistry, Purdue University, 560 Oval Drive, West Lafayette, Indiana 47907

Received April 30, 2007; E-mail: mabuomar@purdue.edu

Abstract: Hydrogen atom transfer (HAT) reactions of (tpfc)MnNTs have been investigated (tpfc = 5,10,-15-tris(pentafluorophenyl)corrole and Ts = *p*-toluenesulfonate). 9,10-Dihydroanthracene and 1,4-dihydrobenzene reduce (tpfc)MnNTs via HAT with second-order rate constants 0.16 ± 0.03 and 0.17 ± 0.01 M^{-1} s^{-1}, respectively, at 22 °C. The products are the respective arenes, $TsNH_2$ and (tpfc)Mn^{III}. Conversion of (tpfc)MnNTs to (tpfc)Mn by reaction with dihydroanthracene exhibits isosbestic behavior, and formation of 9,9′,10,10′-tetrahydrobianthracene is not observed, suggesting that the intermediate anthracene radical rebounds in a second fast step without accumulation of a Mn^{IV} intermediate. The imido complex (tpfc)-Mn^{V}NTs abstracts a hydrogen atom from phenols as well. For example, 2,6-di-*tert*-butyl phenol is oxidized to the corresponding phenoxyl radical with a second-order rate constant of 0.32 ± 0.02 M^{-1} s^{-1} at 22 °C. The other products from imido manganese(V) are $TsNH_2$ and the trivalent manganese corrole. Unlike reaction with dihydroarenes, when phenols are used isosbestic behavior is not observed, and formation of (tpfc)-Mn^{IV}(NHTs) is confirmed by EPR spectroscopy. A Hammett plot for various *p*-substituted 2,6-di-*tert*-butyl phenols yields a V-shaped dependence on σ, with electron-donating substituents exhibiting the expected negative ρ while electron-withdrawing substituents fall above the linear fit (i.e., positive ρ). Similarly, a bond dissociation enthalpy (BDE) correlation places electron-withdrawing substituents above the well-defined negative slope found for the electron-donating substituents. Thus two mechanisms are established for HAT reactions in this system, namely, concerted proton−electron transfer and proton-gated electron transfer in which proton transfer is followed by electron transfer.

Introduction

Metal mediated hydrogen atom transfer (HAT) reactions represent the initial step in many industrially and biologically important processes.[1] Industrially, the Amoco MC oxygenation process as practiced by BP hinges on metal-mediated HAT in the conversion of ∼3 billion pounds of *p*-xylene per year to terephthalic acid (PTA), which is used in the synthesis of polyethylene terephthalate (PET).[2] In biology, oxygen insertion reactions facilitated by biological oxygenases such as cytochrome P450 rely on an initial HAT step according to the radical rebound mechanism.[3] In these systems, the active oxidant, mechanism of HAT, and subsequent fate of the resulting organic radical and metal intermediates are of fundamental interest to synthetic and biological chemists.

For years, the consensus mechanism for cytochrome P450 and its model complexes has been the formation of a terminal oxoiron(IV) porphyrin radical cation (compound I) from the reaction of reduced Fe-poryphyrin with an oxidant such as O_2 or peroxides.[3,4] Traditionally, compound I has been assumed to be the active oxidant in various reaction types that have been observed for P450, such as oxygen insertion, epoxidation, dealkylation, and deamination. However, recent results from enzyme and model studies have pointed to the possibility of multiple oxidative species (Scheme 1).[4−7]

Enzymatically, support for the multiple oxidant hypothesis has been found in drastically varied product types and distributions resulting from protein mutations.[5] For model complexes,

(1) (a) Mayer, J. *Acc. Chem. Res.* **1998**, *31*, 441. (b) Meunier, B.; de Visser, S. P.; Shaik, S. *Chem. Rev.* **2004**, *104*, 3947.
(2) (a) Partenheimer, W. *Catal. Today* **1995**, *23*, *69.* (b) Koshino, N.; Saha, B.; Espenson, J. H. *J. Org. Chem.* **2003**, *68*, 9364. (c) Saha, B.; Koshino, N.; Espenson, J. H. *J. Phys. Chem. A* **2004**, *108*, 425.
(3) Groves, J. T.; Han, Y. Z. In *Cytochrome P450: Structure Mechanisms and Biochemistry*; Ortiz de Monellano, P. R., Ed.; Plenum: New York, 1995; Chapter 1, pp 3−48.
(4) (a) Lee, K. A.; Nam, W. *J. Am. Chem. Soc.* **1997**, *119*, 1916. (b) Primus, J.-L.; Boersma, M. G.; Mandon, D.; Boeren, S.; Veeger, C.; Weiss, R.; Rietjens, I. M. C. M. *J. Biol. Inorg. Chem*. **1999**, *4*, 274. (c) Lee, Y. J.; Goh, Y. M.; Han, S.-Y.; Kim, C.; Nam, W. *Chem. Lett*. **1998**, 837. (d) Kamaraj, K.; Bandyopadhyay, D. *J. Am. Chem. Soc*. **1997**, *119*, 8099. (e) Pratt, J. M.; Ridd, T. I.; King, L. J. *J. Chem. Soc., Chem. Commun*. **1995**, 2297. (f) Machii, K.; Watanabe, Y.; Morishima, I. *J. Am. Chem. Soc*. **1995**, *117*, 6691. (g) Watanabe, Y.; Yamaguchi, K.; Morishima, I.; Takehira, K.; Shimizu, M.; Hayakawa, T.; Orita, H. *Inorg. Chem*. **1991**, *30*, 2581.
(5) (a) Coon, M. J.; Vaz, A. D. N.; McGinnity, D. F.; Peng, H. M. *Drug Metab. Dispos.* **1998**, *26*, 1190. (b) Vaz, A. D. N.; McGinnity, D. F.; Coon, M. J. *Proc. Natl. Acad. Sci. U.S.A.* **1998**, *95*, 3555. (c) Toy, P. H.; Newcomb, M.; Coon, M. J.; Vaz, A. D. N. *J. Am. Chem. Soc.* **1998**, *120*, 9718. (d) Vaz, A. D. N.; Pernecky, S. J.; Raner, G. M.; Coon, M. J. *Proc. Natl. Acad. Sci. U.S.A.* **1996**, *93*, 4644. (e) Toy, P. H.; Dhanabalasingam, B.; Newcomb, M.; Hanna, I. H.; Hollenberg, P. F. *J. Org. Chem.* **1997**, *62*, 9114. (f) Pratt, J. M.; Ridd, T. I.; King, L. J. *J. Chem. Soc., Chem. Commun.* **1995**, 2297.
(6) (a) Nam, W.; Lim, M. H.; Moon, S. K.; Kim, C. *J. Am. Chem. Soc.* **2000**, *122*, 10805. (b) Collman, J. P.; Zeng, L.; Decréau, R. A. *Chem. Commun.* **2003**, 2974.
(7) Song, W. J.; Ryu, Y. O.; Song, R.; Nam, W. *J. Biol. Inorg. Chem.* **2005**, *10*, 294.

Scheme 1. Two Possible Pathways for Cytochrome P450 Oxidations: Rebound Mechanism through Compound I (Pathway 1) and Reaction of Substrate with Oxidant Adduct (Pathway 2)

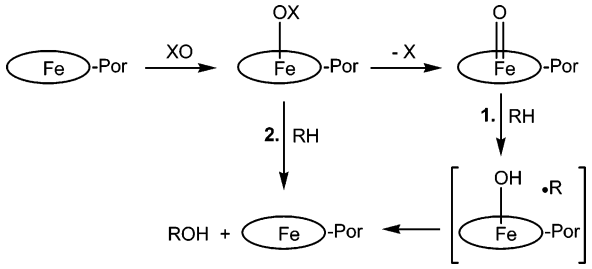

differences in the identity of oxidant,[4f,4e,6] solvent,[4f,6a] and coordination sphere[7] have been shown to affect reactivity. In the case of iron porphyrins, recent results by Collman, Nam, and Que have pointed to an Fe(III)-oxidant adduct as the active species.[8] Furthermore, Goldberg and co-workers have found compelling evidence that the oxidant is an adduct of Mn^{V}═O and PhI═O in expoxidations and sulfoxidations catalyzed by manganese corrolazine.[9]

Our group has recently reported on the analogous aziridination reaction by a manganese corrole and found the active oxidant to be an adduct of the imidomanganese(V) and the iodinane ArI═NTs (ArI = 2-*t*-butylsulfonyliodobenzene). Concurrently, we discovered a competing deactivation pathway by which (tpfc)Mn^{V}NTs (tpfc = 5,10,15-tetrakis(pentafluorophenyl)-corrole) is reduced via hydrogen atom abstraction from the solvent toluene to give $TsNH_2$ and (tpfc)Mn^{III}.[10] Mayer has pioneered the study of HAT reactions by metal−oxo complexes and has also advanced the analogy of metal-based HAT reactions to their organic radical counterparts.[1,11,12] As for porphyrinoid complexes, the work of Goldberg on HAT reactions from phenols to oxomanganese(V) corrolazine is worthy of special mention.[13] Several other reports on hydrogen atom transfer to terminal imido complexes have been reported recently. Borovik et al. have studied HAT to a putative imidoiron(IV) species to give an isolable amidoiron(III), which is stabilized by pendant hydrogen bonds.[14] The second by Holland and co-workers details the reaction chemistry of an iron(III)-imido stabilized by a diketiminate ligand, which abstracts a hydrogen atom intramolecularly from the ketiminate ligand to generate an Fe-(III) amido with formal oxidation of the ligand.[15] HAT has been observed by Warren and co-workers using nickel imidos[16] and by Theopold and co-workers with cobalt imidos.[17] In an interesting twist, an example of the reverse reaction has recently been reported by Smith and co-workers, in which the synthesis of a cobalt imido species is achieved by reaction of cobalt amido with a phenoxyl radical.[18] Also worthy of mention is the recent work of Peters and Chirik, who have activated H_2 with iron imido compounds.[19]

Herein, we report on hydrogen atom transfer reactions of an imidomanganese(V) corrole complex. The reaction occurs via two subsequent HAT reactions, the second of which is fast. We have found that the initial rate-determining HAT reaction can occur by two different pathways: a concerted proton−electron transfer or a proton transfer followed by electron transfer (PT−ET).

Results and Discussion

Reactivity and Kinetics of (tpfc)MnNTs toward HAT Substrates. The terminal tosylimido complex of manganese corrole is formed by the reaction of (tpfc)Mn (**1**) with ArINTs (Ar = 2-*tert*-butylsulfonylbenzene), eq 1. In addition to its role as an aziridination catalyst, **2** reacts via HAT with solvents that possess a thermodynamically suitable hydrogen atom, such as toluene.[10] To further explore this reactivity of **2**, we examined its reduction by hydrogen atom donor substrates such as dihydroarenes and 2,6-di-*tert*-butyl phenols, eqs 2 and 3.

(tpfc)Mn (**1**) + ArINTs → (tpfc)MnNTs (**2**) + ArI (1)

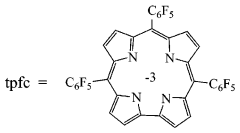

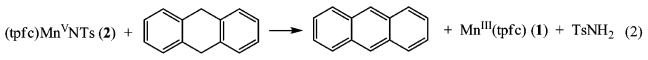

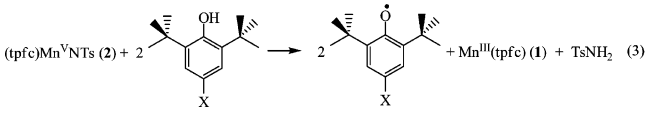

Both reactions proceed to completion, and all products as shown have been identified and quantified to greater than 90% yield. Product **1** is detected and quantified by absorption spectroscopy. Diamagnetic organic products, anthracene, and $TsNH_2$ were detected and quantified by ^1H NMR and gas chromatography. Phenoxyl radical was detected by EPR spectroscopy. Quantification of phenoxyl radical was done indirectly by the reaction of **2** with 2-*tert*-butyl-4-methylphenol, which couples to give the biaryl product (Scheme 2).[13,20]

Under conditions of excess phenol or dihydroarene, the HAT reaction follows pseudo-first-order kinetics and affords k_ψ that exhibits first-order dependence on the excess substrate concentration (dihydroarene or phenol). Typical kinetic data are

(8) (a) Nam, W.; Choi, S. K.; Lim, M. H.; Rohde, J.-U.; Kim, I.; Kim, J.; Kim, C.; Que, L., Jr. *Angew. Chem., Int. Ed.* **2003**, *42*, 109. (b) Collman, J. P.; Chien, A. S.; Eberspacher, T. A.; Brauman, J. I. *J. Am. Chem. Soc.* **2000**, *122*, 11098. (c) Nam, W.; Lim, M. H.; Lee, H. J.; Kim, C. *J. Am. Chem. Soc.* **2000**, *122*, 6641.
(9) Wang, S. H.; Mandimutsira, B. S.; Todd, R.; Ramdhanie, B.; Fox, J. P.; Goldberg, D. P. *J. Am. Chem. Soc.* **2004**, *126*, 18.
(10) Zdilla, M. J.; Abu-Omar, M. M. *J. Am. Chem. Soc.* **2006**, *128*, 16971.
(11) (a) Tahmassebi, S. K.; McNeil, W. S.; Mayer, J. M. Organometallics **1997**, *16*, 5342−5353. (b) Wang, K.; Mayer, J. M. *J. Org. Chem.* **1997**, *62*, 4248. (c) Cook, G. K.; Mayer, J. M. *J. Am. Chem. Soc.* **1995**, *117*, 7139. (d) Gardner, K. A.; Mayer, J. M. *Science* **1995**, *269*, 1849. (e) Cook, G. K.; Mayer, J. M. *J. Am. Chem. Soc.* **1994**, *116*, 1855. (f) Cook, G. K.; Mayer, J. M. *J. Am. Chem. Soc.* **1994**, *116*, 8859. (g) Conry, R. R.; Mayer, J. M. *Organometallics* **1993**, *12*, 3179. (h) Conry, R. R.; Mayer, J. M. *Organometallics* **1991**, *10*, 3160. (i) Conry, R. R.; Mayer, J. M. *Inorg. Chem.* **1990**, *29*, 4862.
(12) Rhile, I. J.; Markle, T. F.; Nagao, H.; DiPasquale, A. G.; Lam, O. P.; Lockwood, M. A.; Rotter, K.; Mayer, J. M. *J. Am. Chem. Soc.* **2006**, *128*, 6075.
(13) Lansky, D. E.; Goldberg, D. P. *Inorg. Chem.* **2006**, *45*, 5119.
(14) Lucas, R. L.; Powell, D. R.; Borovik, A. S. *J. Am. Chem. Soc.* **2005**, *127*, 11596.
(15) Eckert, N. A.; Vaddadi, S.; Stoian, S.; Lachicotte, R. J.; Cundari, T. R.; Holland, P. L. *Angew. Chem., Int. Ed.* **2006**, *45*, 6868.
(16) Kogut, E.; Wiencko, H. L.; Zhang, L.; Cordeau, D. E.; Warren, T. H. *J. Am. Chem. Soc.* **2005**, *127*, 11249.
(17) (a) Shay, D. T.; Yap, G. P. A.; Zakharov, L. N.; Rheingold, A. L.; Theopold, K. H. *Angew. Chem., Int. Ed.* **2005**, *44*, 1508. (b) Shay, D. T.; Yap, G. P. A.; Zakharov, L. N.; Rheingold, A. L.; Theopold, K. H. *Angew. Chem., Int. Ed.* **2006**, *45*, 7870.
(18) Cowley, R. E.; Bontchev, R. P.; Sorrell, J.; Sarracino, O.; Feng, Y.; Wang, H.; Smith, J. M. *J. Am. Chem. Soc.* **2007**, *129*, 2424.
(19) (a) Brown, S. D.; Peters, J. C. *J. Am. Chem. Soc.* **2004**, *126*, 4538. (b) Bart, S. C.; Lobkovsky, E.; Bill, Eckhard; Chirik, P. J. *J. Am. Chem. Soc.* **2006**, *128*, 5302.
(20) Liguori, L.; Bjørsvik, H.-R.; Fontana, F.; Bosco, D.; Galimberti, L; Minisci, F. *J. Org. Chem.* **1999**, *64*, 8812.

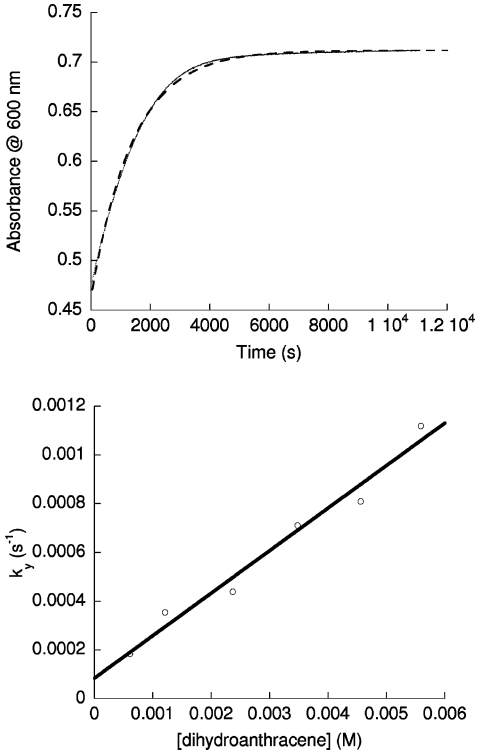

Figure 1. Kinetic data for abstraction of hydrogen atoms from excess dihydroanthracene by compound **2** in benzene solvent at 22 °C. The top panel shows (—) data, (---) fit. $[\mathbf{2}]_0 = 5 \times 10^{-5}$ M; [dihydroanthracene] = 3.5×10^{-3} M; k_ψ from fit = $7.12 \pm 0.02 \times 10^{-4}$ s^{-1}; $R = 0.9991$. The bottom panel shows a plot of k_ψ vs [dihydroanthracene]. Data designated by points; fit designated by line. k from fit = 0.175 ± 0.014 M^{-1} s^{-1}; $R = 0.986$.

Scheme 2. Aryl Coupling of 6-Unsubstituted Phenoxyl Radicals

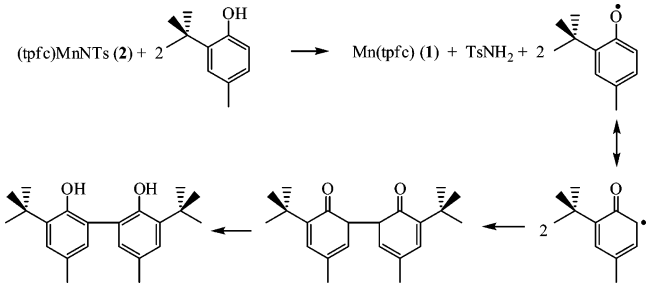

displayed for the reaction of **2** with dihydroanthracene (DHA) in Figure 1. A comment regarding the *y*-intercept of k_ψ versus [substrate] plots is in order. Most investigated substrates when dried thoroughly give negligible intercepts within statistical error. 3,5-Di-*t*-butyl-4-hydroxyacetophenone and a couple of the deuterated phenols are the exception. They must contain either residual moisture or a small impurity that was not totally removed in the purification process, which gives rise to an appreciable *y*-intercept. Nevertheless, the kinetics are reproducible and the contribution from the *y*-intercept amounts to no more than 20% of the overall rate. Therefore, the rate law in eq 4 can be simplified to an overall second-order equation.

$$-\mathrm{d}[\mathbf{2}]/\mathrm{d}t = (k[\text{substrate}] + b)[\mathbf{2}] \cong k[\mathbf{2}][\text{substrate}] \quad (4)$$

A significant deuterium kinetic isotope effect (KIE) was observed for both dihydroanthracene (DHA) as well as 2,4,6-tri-*tert*-butylphenol. A hydrogen KIE is consistent with a rate-limiting hydrogen atom transfer mechanism.[1] Rate constants, KIE values, and activation parameters are summarized in Table 1.

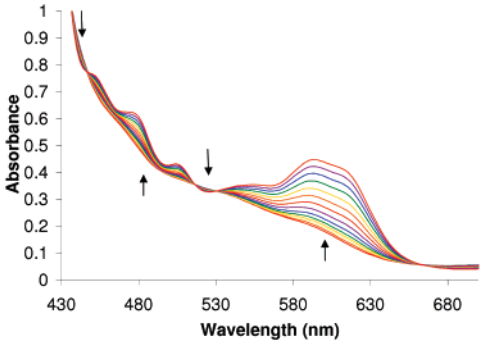

Figure 2. Reaction of **2** and DHA monitored by absorption spectroscopy in benzene: $[\mathbf{2}] = 4.8 \times 10^{-5}$ M; [dihydroanthracene] = 1.67×10^{-3} M; $T = 22$ °C; scan interval = 2 min.

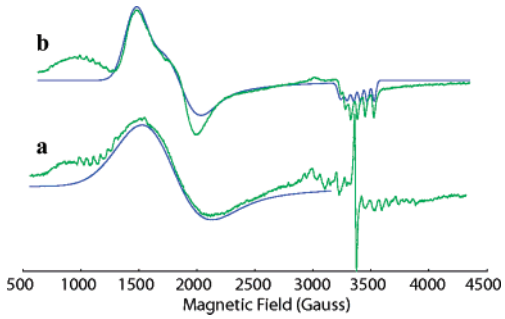

Figure 3. (a) EPR spectrum of amido intermediate (tpfc)Mn^{IV}(NHTs) (**3**) in toluene glass at 5 K with signals at $g_\perp = 4$ and $g_\parallel = 2$ (only the $g_\perp$ region is simulated because of the $g_\parallel$ being obscured by other $g = 2$ signals and by subtraction of a $g = 2$ baseline signal in the instrument). (b) EPR spectrum of $[(\text{tpfc})\text{Mn}^{IV}]^+$ (**5**) in toluene glass at 5 K with $g_x = 4.57$, $g_y = 3.60$, and $g_z = 1.995$. Experimental data is shown in green with spectral simulation in blue. Other signals are Mn(III) at $g = 8$, phenoxyl radical at $g = 2.003$, and a trace amount of $S = {}^1/_2$ Mn dimer resulting from hydrolysis by trace H_2O (16-line signal at $g = 2$). Modulation frequency = 100 kHz; Modulation amplitude = 7.182 G; microwave frequency = 9.44 GHz; microwave power = 10 mW.

Table 1. Rate Constants, KIE, and Activation Parameters for Hydrogen Atom Abstraction by Compound **2**

substrate		k $M^{-1}s^{-1}$	kH/kD (KIE)[a]	$\Delta H^\ddagger$ kJ mol^{-1} [a]	$\Delta S^\ddagger$ J mol^{-1} K^{-1} [a]
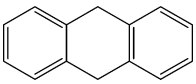		0.17 ± 0.01	3.5	nd	nd
		0.16 ± 0.03	nd	nd	nd
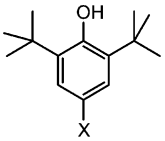	X = OMe	25 ± 1	4.3	32.3(5)	−106(2)
	X = tBu	1.15 ± 0.06	5.1	nd	nd
	X = CH3	1.9 ± 0.1	nd	39(2)	−110(7)
	X = H	0.32 ± 0.02	nd	40(4)	−114(14)
	X = Ac	0.31 ± 0.02	nd	nd	nd
	X = CHO	0.59 ± 0.05	nd	42(1)	−114(4)
	X = CN	1.5 ± 0.1	3.0	32(4)	−157(15)

[a] nd = not determined.

Intermediacy of Mn(IV) Amido Complex. Given that the tosylimido complex is converted completely to the amine

Scheme 3. Reactivity of **2** with Different Substrates

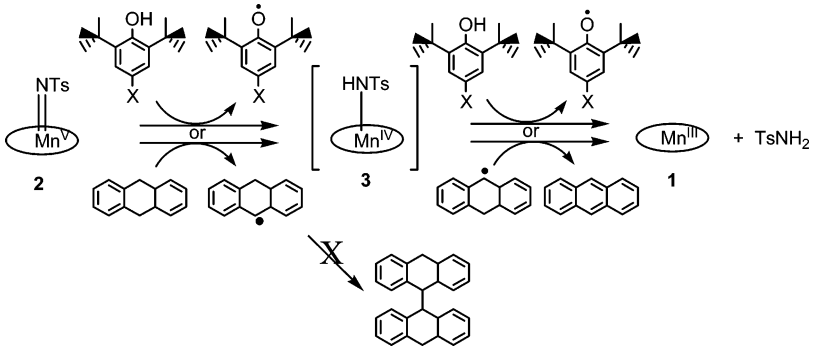

product $TsNH_2$, reactions 2 and 3 undergo two hydrogen abstraction steps, passing through a putative manganese(IV) amido complex, (tpfc)Mn^{IV}(NHTs) (**3**). However, the reaction of **2** with DHA shows tight isosbestic conversion between **2** and **1** (Figure 2). This observation implies no significant intermediate buildup, and the second hydrogen atom abstraction must be fast. A fast second HAT step is consistent with the single-phase kinetic profiles observed for DHA and first-order dependence on substrate. Attempts to detect a "short-lived" Mn(IV) amido intermediate by EPR spectroscopy were unsuccessful.[21] Additional evidence for this fast second step is the absence of coupled organic product 9,9′,10,10′-tetrahydro-9,9′-bianthracene, which suggests that the initially formed radical does not escape, accumulate, and couple (Scheme 3).[22] Rather, the carbon radical rebounds with a second HAT reaction to give anthracene exclusively. In comparison, in a report by Borovik[14] the reaction of a putative iron(IV) imido with DHA was found to terminate after a single HAT event to give iron(III) amido and DHA•, which couples to afford the tetrahydrobianthracene.

In the case of HAT from phenol substrates, UV−vis spectra do not show isosbestic conversion between **2** and **1** (Supporting Information). This result suggests that there is buildup of a third species in the reaction with phenols, eq 3. After careful consideration, we realized that this intermediate buildup can be easily reconciled. Phenol substrates, unlike dihydroarenes, have only one available hydrogen atom for abstraction. Even if the second abstraction is faster than the first, the resulting phenoxyl radical, which may stabilize **3** by hydrogen bonding, must first diffuse into solution to allow a second phenol molecule to approach the putative manganese(IV) amido complex **3** for a second HAT reaction. Attempts to trap the presumed intermediate (tpfc)Mn^{IV}(NHTs) (**3**) by addition of substoichiometric amounts of phenol to **2** were unsuccessful, resulting in complete conversion to **1**, presumably by a subsequent HAT from solvent under limiting phenol conditions. However, the Mn(IV) intermediate **3** was successfully trapped by freeze-quenching the reaction with phenol substrates and was observed by EPR spectroscopy (Figure 3). In addition to the phenoxyl radical signal at $g = 2.003$, the broad Mn(III) signal at $g = 8$, and that of trace manganese dimer at $g = 2.05$,[10,23] the prominent axial signal of Mn(IV) with $g_\perp$ at 4 and a partially buried $g_\parallel$ near $g = 2$ are apparent. These features are comparable to axial spectra of previously reported Mn(IV) porphyrins.[24] The concentration of **3** was determined to be ca. 10 μM by double integration and by comparison to the intensity of the comparable $S = {}^3/_2$ system (tpfc)Mn^{IV}Br.[25] Thus, our system provides a rare example of a two-step oxidation rebound mechanism where the metal intermediate can be observed spectroscopically by the proper selection of a substrate that cannot rebound, namely phenol. These mechanistic findings are summarized in Scheme 3.

Linear Free Energy Relationships (LFER): Evidence for Multiple Mechanistic Pathways. To gather further insight for the HAT mechanism, we constructed a Hammett plot using substituted phenol substrates. All substituted phenols studied give rise to the same rate law (eq 4) and reaction products, namely **1**, $TsNH_2$, and the corresponding phenoxyl radical. In performing the Hammett LFER, we expected to find a general negative ρ similar to that observed by Goldberg for the HAT reaction of phenol substrates with oxomanganese(V) corrolazines.[13] What we observed instead was a V-shaped Hammett plot as illustrated in Figure 4a. While electron-donating substituents show the expected negative slope (reaction constant, ρ), electron-withdrawing substituents appear significantly above the established trend (positive ρ). A Hammett plot such as this is indicative of a change in mechanism on either side of the vertex. To support the notion of two mechanistic possibilities, we also plotted the log k versus bond dissociation enthalpy (BDE)[26] (Figure 4b). Again, electron-donating substitutents show a negative slope comparable to that seen by Goldberg,[13] but the electron-withdrawing acetyl and cyano substituents break the correlation. A scatter plot of the second-order rate constants versus pK_a values as determined by Cohen and Jones[27] does not give a clear correlation, but demonstrates that the electron-

(21) After addition of dihydroanthracene to a solution of **2**, the reaction was quenched by freezing in liquid nitrogen and analyzed by EPR spectroscopy at 5 K. The tube was repeatedly thawed to allow continuation of the reaction and refrozen for analysis. An axial Mn^{IV} signal was never observed.

(22) While it is possible that the weak DHA• C−H bond is the sole reason for the absence of coupled product, the scenario is unlikely given that the radical was seen by Borovik[14] to escape the solvent cage and couple, even in the more viscous dimethylacetamide solvent. The likelihood of benzene solvent cage completely preventing any radical coupling is quite small.

(23) The 16-line signal at $g = 2.05$ is due a small amount of a $S = {}^1/_2$ manganese μ-oxo dimer resulting from minor hydrolysis of terminal imido.[10]

(24) Camenzind, M. J.; Hollander, F. J.; Hill, C. L. *Inorg. Chem.* **1983**, *22*, 3776.

(25) Golubkov, G.; Bendix, J.; Gray, H. B.; Mahammed, A.; Goldberg, I.; DiBilio, A. J.; Gross, Z. *Angew. Chem., Int. Ed.* **2001**, *40*, 2132.

(26) (a) For phenols with X = OMe, ^{t}Bu, Me, and H, the BDE values as measured by Pedulli were used: Lucarini, M.; Pedrielli, P.; Pedulli, G. F.; Cabiddu, S.; Fattuoni, C. *J. Org. Chem.* **1996**, *61*, 9259. (b) For X = CN, Ac the BDE values were approximated using the ΔBDEs reported by Bordwell: Bordwell, F. G.; Cheng, J.-P. *J. Am. Chem. Soc.* **1991**, *113*, 1736. While these BDE values are not exact, 18 cases were examined by Pedulli (reference 26a) and were shown to be highly accurate with one exception for 4-methoxytetramethylphenol, which was attributed to steric reorientation of the oxygen lone pair orbital. These approximations are therefore sufficient to establish BDE trends.

(27) Cohen, L. A.; Jones, W. M. *J. Am. Chem. Soc.* **1963**, *81*, 3397.

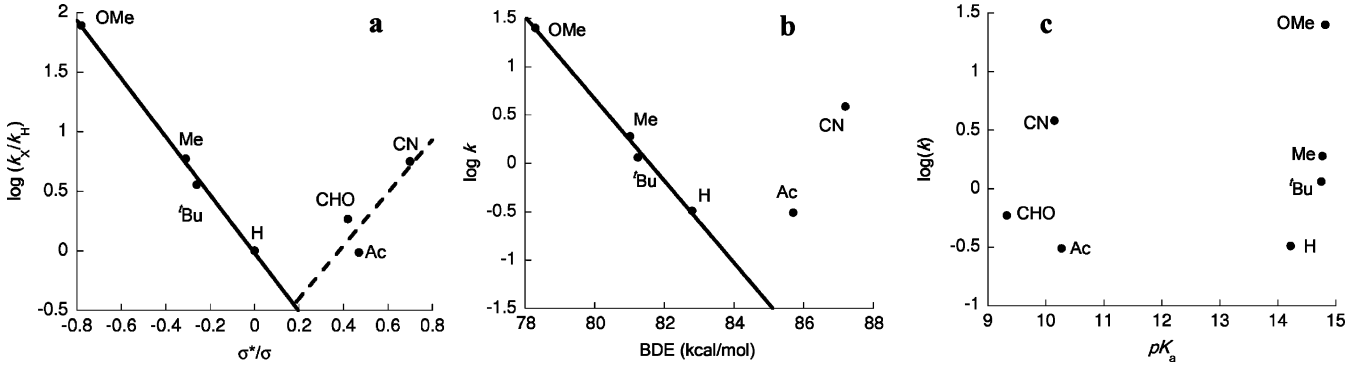

Figure 4. Linear free energy correlations for HAT reactions. (a) Hammett substituent plot for reaction of **2** with 2,6-di-*tert*-butyl phenols. For electron-donating substituents (left), $\rho = -2.4 \pm 0.1$. (b) BDE correlation with log k; slope $= -0.42 \pm 0.02$. (c) Scatter plot of log k vs phenol pK_a.

Scheme 4. Mechanistic Possibilities for Positive Hammett Reaction Constant in Hydrogen Atom Transfer

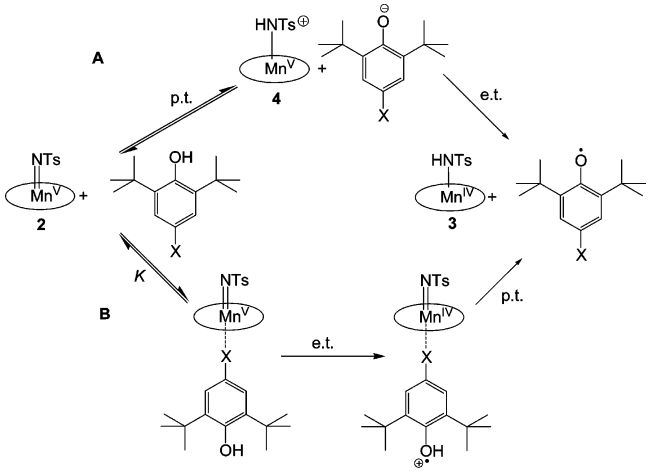

withdrawing substitutents lie in a very different pK_a regime when compared to the electron donating groups (Figure 4c).

Further confirmation of the difference in mechanism was sought in the determination of activation parameters for substrates on either side of the vertex (Table 1). However, as the entropy of activation increases for the series, the enthalpy of activation does not change much. The isokinetic plot of $\Delta H^{\ddagger}$ versus $\Delta S^{\ddagger}$ for phenol substrates (Supporting Information) does not show a correlation. All substrates have similar activation parameters within error with the exception of the Hammett extremes (i.e., X = OMe, CN).

In considering alternative mechanisms for phenols with electron-withdrawing groups, the following requisites must be satisfied: First, the proposed mechanism must be expected to result in a positive Hammett reaction constant ρ. If this condition is not satisfied, the proposed mechanism would also have to be in effect for electron-donating substituents and there would be no vertex in the Hammett plot. Second, the end products and intermediate must be identical to the concerted proton−electron transfer mechanism, namely, phenoxyl radical **1** and intermediate **3**.

We have considered two mechanisms that satisfy these conditions. These are shown in Scheme 4. The first is proton transfer followed by electron transfer (A), commonly referred to as proton-gated electron transfer (PT−ET).[28] As more withdrawing substituents are employed, the acidity of the phenolic proton increases. It is therefore reasonable that in moving left to right on the Hammett plot a point is encountered where protonation of the terminal imido ligand becomes feasible and more favored than concerted proton−electron transfer. The second proposed mechanism (B) takes into consideration the increasing coordinating ability of the electron-withdrawing substituents. In this remote attack mechanism,[29] the phenol ligates to the metal center via the *p*-substituent, allowing for inner-sphere (through-bond) electron transfer, followed by (most likely fast) proton transfer from the protonated phenoxyl radical. The reaction rate via pathway B relies on the equilibrium constant K, hence, the ligand strength of the substituent group. Thus, cyano would be expected to be faster than aldehyde.

The second mechanism (B) can be ruled out on the basis of the presence of a primary hydrogen KIE for deutero versus protio 2,6-di-*t*-butyl-4-cyanophenol (Table 1). Since neither the equilibrium constant K, nor the rate-limiting electron transfer involve the hydrogen atom, mechanism B cannot result in a KIE. Thus, mechanism A, PT−ET is the most likely alternate mechanism for the reaction. Additional support for this mechanism was found in the feasible protonation of compound **2**. Mechanism A suggests that **2** should be a Brønsted base capable of accepting a proton. Addition of anhydrous trifluoroacetic acid to **2** (eq 5) results in a new species, which is identified by mass spectrometry as the protonated imidomanganese(V), (tpfc)Mn(NHTs)$^+$ (**4**, m/z =1017.53, calcd = 1018).

$$(\text{tpfc})\text{Mn}^{\text{V}}\text{NTs}\ (\mathbf{2}) + \text{CF}_3\text{COOH} \rightarrow [(\text{tpfc})\text{Mn}^{\text{V}}(\text{NHTs})]^+ [\text{CF}_3\text{COO}]^-(\mathbf{4}[\text{CF}_3\text{OO}]^-) \quad (5)$$

This species is short-lived, and is only detected within the few seconds after it is generated, as it rapidly picks up a hydrogen atom, probably from the solvent, to give $TsNH_2$ and [(tpfc)Mn$^{\text{IV}}$]$^+$ (**5**). The higher reactivity of the protonated imide complex **4** in comparison to **2** is consistent with our mechanistic proposal (Scheme 4A).

$$[(\text{tpfc})\text{Mn}^{\text{V}}(\text{NHTs})]^+\ (\mathbf{4}) \xrightarrow{[\text{H}]} [(\text{tpfc})\text{Mn}^{\text{IV}}]^+\ (\mathbf{5}) + \text{TsNH}_2 \quad (6)$$

The appearance of $TsNH_2$ is confirmed by ^{1}H NMR (50% yield), and **5** is characterized by EPR, UV−vis, and mass

(28) Chen, K.; Hirst, J.; Camba, R.; Bonagura, C. A.; Stout, C. D.; Burgess, B. K.; Armstrong, F. A. *Nature* **2000**, *405*, 814.

(29) (a) Haim, A. *Acc. Chem. Res.* **1975**, *8*, 264. (b) Fraser, R. T. M.; Taube, H. *J. Am. Chem. Soc.* **1961**, *83*, 2239.

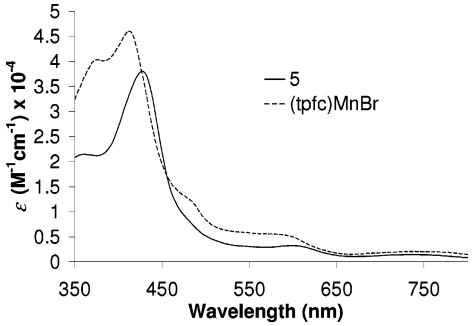

Figure 5. Comparative absorption spectra of compound **5** (solid line) and (tpfc)Mn^{IV}Br (dashed line) in benzene.

spectrometry. The mass spectrum exhibits an overwhelming signal at $m/z = 848$, corresponding to **5** (see Supporting Information). The EPR spectrum exhibits an $S = {}^3/_2$ rhombic Mn(IV) signal that is different from that of **3** (Figure 3b). Last, the absorption spectrum bears a striking resemblance to the previously reported Mn(IV) corrole (tpfc)MnBr (Figure 5).[25] **5** reacts readily with phenoxides to yield **1** and phenoxyl radical according to absorption and EPR spectroscopies, respectively.

$$[(\text{tpfc})\text{Mn}^{\text{IV}}(\mathbf{5})]^+ + \text{ArO}^- \rightarrow (\text{tpfc})\text{Mn}^{\text{III}}(\mathbf{1}) + \text{ArO}^\bullet \qquad (7)$$

Only 1 equiv of trifluoroacetic acid is needed to convert nearly all of **2** to **5**, with very little spectral change (<5%) observed with additional equivalents of trifluoroacetic acid. This result demonstrates the capability of **2** as a proton acceptor, a result consistent with our previous report that the imido ligand of **2** is bent with a nitrogen lone pair and Mn═NTs double-bond character.[10] As expected, the resulting Mn(V) amido (**5**) is highly reactive toward reduction chemistry, which further validates the likelihood of the PT−ET mechanism for electron-poor phenols.

Conclusions

HAT reactions with terminal tosylimidomanganese(V) corrole proceed in a two-step mechanism for which the rate-determining step is the first hydrogen atom transfer resulting in an intermediate tosylamidomanganese(IV) complex, which can be detected by EPR spectroscopy if the hydrogen-donating substrate is a non-rebounding substrate such as 2,6-di-*t*-butylphenol. In the case of dihydroarenes, the arene radical rebounds with Mn(IV) to give arene and Mn(III) at a faster rate than diffusing into solution to react with another equivalent of radical or Mn(V) imido. For reactions with 4-substituted 2,6-di-*tert*-butylphenols, the rate-determining initial step can proceed by two mechanisms. In the case of electron-donating substituents, the reaction proceeds through concerted proton−electron transfer, while in the case of electron-withdrawing substituents, the reaction proceeds via PT−ET. In these examples the substrate type (namely phenol) is the same, yet the reaction pathways are dependent upon the acidity of the phenolic proton. These findings demonstrate that the substrate pK_a is an important consideration not only for the rate of metal-mediated HAT reactions, but for the molecular mechanism as well.

Experimental

General. All operations were carried out under inert atmosphere using standard glovebox and Schlenk line techniques except where otherwise noted. Benzene, toluene, and *n*-pentane were distilled from sodium-benzophenone ketyl. Solvents were degassed and stored over activated 4-Å molecular sieves in a glovebox for 24 h prior to use. NMR solvents and ethanol-d_1 were purchased from Cambridge Isotope Laboratories. NMR solvents were stored over activated 4-Å molecular sieves for 24 h prior to use. 2,6-Di-*tert*-butyl-4-X-phenol compounds were purchased from Aldrich, TCI, Alfa Aesar, or Acros. 9,10-Dihydroanthracene and 1,4-cyclohexadiene (dihydrobenzene) were purchased from Aldrich. Sodium metal was obtained from Fluka. All purchased chemicals were used as obtained from the manufacturers unless specified otherwise. (tpfc)Mn (**1**) was prepared according to a previous report.[10] 2-(*t*-Butylsulfonyl)(*p*-toluene-sulfonyliminoiodo)-benzene was prepared by the method of Protasiewicz.[30] 9,10-Dihydroanthracene-d_4 was prepared by the method of Mayr.[31] Lithium 2,6-di-*tert*-butyl-4-cyanophenoxide was prepared according to the method of Henderson et al.[32]

UV−vis spectra were recorded on a Shimadzu UV-2501PC scanning spectrophotometer. NMR spectra were obtained on Inova/Varian 300 MHz spectrometer. Gas chromatography was carried out on an Agilent Technologies 6890N Network GC system with a J&W Scientific DB-5 capilary column. Oven temperature was ramped from 70 to 150 °C at 25 °/min, then from 150 to 230 at 15 °/min in constant flow mode at 2.5 mL/min. Kinetics experiments were performed using an Applied Photophysics SX.18MV stopped-flow analyzer or a Shimadzu UV-2501PC scanning spectrophotometer in 3 mL quartz cells with 1 cm path length. EPR spectra were recorded on a Bruker ESP 300E EPR spectrometer equipped with an hp 5350B microwave frequency counter, an Oxford ITC4 temperature controller, and a VC[40] gas flow controller (for liquid He) and a Eurotherm temperature control unit (liquid N_2). Data fitting was carried out using KaleidaGraph. EPR spectra were simulated using the Easyspin[33] program for MATLAB.

Phenols were dried by dissolving in a minimal amount of dry solvent (hexanes for X = H, Me, ^{t}Bu; CH_2Cl_2 for X = CHO, Ac, OMe) and storing over activated molecular sieves for 24 h. After removing sieves, the compounds were recrystalized from their respective solvents (volume reduction for X = H, Me, ^{t}Bu; and by addition of hexanes for X = CHO, Ac, OMe). Solids were filtered and rinsed with a minimum of cold *n*-pentane and dried in vacuo.

Synthesis of 4-X-2,6-*t*-$Bu_2C_6H_2OD$. Deuterated phenols were prepared by an adaptation of the method of Mayr[31] for the deuteration of 9,10-dihydroanthracene. Under an inert atmosphere, Na metal (1 g, 44 mmol) was dissolved in 20 mL of ethanol-*d*. To this was added 4-X-2,6-*t*-$Bu_2C_6H_2OH$ (ca. 6−9 mmol). After 10 h of stirring, the solvent volume was reduced in vacuo to 8 mL, and 20 mL of D_2O was added yielding a light-yellow precipitate. The solid was cooled to 0 °C, filtered, and dried under vacuum. Degree of deuteration was determined by the integration of the phenol proton peak (300 MHz ^{1}H NMR, C_6D_6). Degree of deuteration: X = MeO at 4.5 ppm, 88% deuteration, 94% yield; X = CN at 5.2 ppm, 85% deuteration, 40% yield; X = ^{t}Bu at 3.9 ppm, >99% deuteration, 97% yield.

Kinetic Studies. Reaction of (tpfc)Mn^VNTs with Substrates. General Procedures. Kinetic traces for the reaction between (tpfc)-Mn^VNTs and phenol or dihydroarene substrates were obtained under pseudo-first-order conditions with excess substrate. Reactions were monitored by UV−vis spectroscopy or a stopped-flow analyzer by following the increase in the absorbance of the Q-band peak for (tpfc)-Mn^{III} at 600 nm. Stock solutions were prepared and stored under an inert atmosphere with benzene as the solvent. Prior to each kinetic run, fresh solutions of (tpfc)MnNTs, **2**, ($3-4 \times 10^{-5}$ M) were prepared by reacting 50 μM of (tpfc)Mn^{III} and limiting amount ($3-4 \times 10^{-5}$ M) of 2-(*t*-butylsulfonyl)(*p*-toluene-sulfonyliminoiodo)benzene for 5 min. Different amounts of a stock solution of the phenol substrate were added

(30) Macikenas, D.; Skrzypczak-Jankun, E.; Prostasiewicz, J. D. *J. Am. Chem. Soc.* **1999**, *121*, 7164.
(31) Mayr, H.; Lang, G.; Ofial, A. R. *J. Am. Chem. Soc.* **2002**, *124*, 4076.
(32) MacDougall, D. J.; Noll, B. C.; Kennedy, A. R.; Henderson, K. W. *Dalton Trans.* **2006**, 1875.
(33) Stoll, S.; Schweiger, A. *J. Magn. Reson.* **2006**, *178*, 42.

to initiate the reaction. Four to six different concentrations were used for each substrate, and pseudo-first-order rate constants (k_ψ) were determined at each concentration. Plots of k_ψ versus [substrate] yielded the second-order rate constants k. Metal syringes were avoided for all phenol kinetics because of our observation that contact with metal surfaces enhances reaction rates for some phenols.

Reaction of (tpfc)Mn^{V}NTs with 4-X-2,6-*t*-Bu$_2$C$_6$H$_2$OH (X = ^{t}Bu, OCH$_3$, Ac, or CHO, or CHO) and 4-*t*-Bu-2,6-*t*-Bu$_2$C$_6$H$_2$OD. Kinetic experiments were carried out according to the general procedure using UV−vis spectroscopy (stop flow for OCH_3). (tpfc)Mn^{V}NTs (ca. $2-4 \times 10^{-5}$ M) reacted with varied concentrations of phenol substrate (2×10^{-3} to 2×10^{-2} M).

Reaction of (tpfc)Mn^{V}NTs with 2,4,6-*t*-Bu$_2$C$_6$H$_2$OD/2,6-*t*-Bu$_2$C$_6$H$_2$OH. Kinetic experiments were carried out according to the general procedure using UV−vis spectroscopy. (tpfc)Mn^{V}NTs (ca. 2×10^{-5} M) reacted with varied concentrations of phenol substrate (3.8−38 mM).

Reaction of (tpfc)Mn^{V}NTs with 4-CN-2,6-*t*-Bu$_2$C$_6$H$_2$OH. Kinetic experiments were carried out according to the general procedure using UV−vis spectroscopy. (tpfc)Mn^{V}NTs (ca. 2×10^{-5} M) reacted with varied concentrations of phenol substrate (0.46−13 mM).

Reaction of (tpfc)Mn^{V}NTs with 9,10-Dihydroanthracene and 1,4-Cyclohexadiene. Kinetic experiments were carried out according to the general procedure using UV−vis spectroscopy. (tpfc)Mn^{V}NTs (ca. 5×10^{-5} M) reacted with varied concentrations of 9,10-dihydroanthracene (6.1×10^{-4} to 5.6×10^{-3} M) or 1,4-cyclohexadiene (4.1×10^{-3} to 3.8×10^{-2} M).

Activation Parameters Studies. Kinetic traces were obtained by monitoring absorbance at 600 nm at varied temperatures for the reaction of (tpfc)Mn^{V}NTs with excess phenol under pseudo-first-order conditions in accordance with the general procedure described above. Reactions were performed at four different temperatures (7−60 °C), and second-order rate constants (k) were determined at each temperature. The Eyring plot of ln(k/T) versus 1/T yielded $\Delta H^{\ddagger}$ and $\Delta S^{\ddagger}$ values.

Detection of (tpfc)Mn^{IV}(NHTs) Intermediate (3) by EPR Spectroscopy. (tpfc)Mn^{V}NTs (**2**) was generated by the addition of 1 mg of 2-(*t*-butylsulfonyl)(*p*-toluene-sulfonyliminoiodo)benzene to a solution of 1 mg of (tpfc)Mn (**1**) in 1 mL of toluene. To initiate the HAT reaction, 1.25 μL of a 0.1 M stock solution of 2,6-di-*tert*-butylphenol was added to 0.25 mL of solution of **2**. An immediate color change to green ensued, and the reaction was quickly quenched by immersion into liquid N_2. The sample was analyzed by EPR at 5 K and showed the characteristic $S = {}^3/_2$ spectrum for **3**. Modulation frequency = 100 kHz; modulation amplitude = 7.182 G; microwave frequency = 9.44 GHz; microwave power = 10 mW.

An identical test for **3** using dihydroanthracene in place of 2,6-di-*tert*-butyl phenol did not yield the signature for **3**.

Detection of [(tpfc)Mn(NHTs)]$^{+}$(4) by Mass Spectrometry. To a solution of 1 mg (tpfc)Mn (**1**, 1 μmol) in 0.25 mL of benzene, 1 μL of anhydrous trifluoroacetic acid was added (no color change). This solution was added to 1 mg (2 mmol) of 2-(*t*-butylsulfonyl)(*p*-toluene-sulfonyliminoiodo)benzene to afford a color change from green to green−yellow. This solution was analyzed immediately by ESI mass spectrometry: observed m/z = 1017.53; theoretical for (tpfc)Mn(NHTs)$^{+}$ m/z = 1018.

Generation and Detection of [(tpfc)Mn^{IV}]$^{+}$(5) by Absorption Spectroscopy. To 3 mL of a 3.3×10^{-5} M solution of (tpfc)Mn (**1**), 59 μL of a 1.7×10^{-3} M stock solution of 2-(*t*-butylsulfonyl)(*p*-toluene-sulfonyliminoiodo)benzene was added to generate **2**. This solution was titrated by μL additions of 0.15 M anhydrous trifluoroacetic acid in benzene to give the spectrum of **5**.

Generation and Detection of [(tpfc)Mn^{IV}]$^{+}$(5) by EPR Spectroscopy. To 1 mL of a 1 mM solution of **1** in toluene, 2 equiv of solid 2-(*t*-butylsulfonyl)(*p*-toluene-sulfonyliminoiodo)benzene was added, and the solution was stirred until red−brown (ca. 1 min). A 0.25 mL aliquot of this solution was added to an EPR tube containing 20 μL of trifluoroacetic acid/benzene 1:1000 (1 equiv) to afford a color change to brown/green. The EPR tube was frozen in liquid nitrogen and analyzed by EPR.

Reaction of [(tpfc)Mn^{IV}]$^{+}$ (5) with Phenoxide. An amount of 3 mL of a 5×10^{-5} M solution of **1** was stirred with 2 mg of PhINTs until brown/orange in color. This solution was decanted to a new vial and 12 μL of benzene/trifluoroacetic acid 1:1000 was added to give a color change to green/brown. This was added to a new vial containing 1 mg of lithium 2,6-di-*tert*-butyl-4-cyanophenoxide[32] to afford a color change to green. Analysis by absorption spectroscopy identifies the manganese product as **1**. The experiment was repeated in toluene and analyzed by EPR spectroscopy to confirm the appearance of phenoxyl radical, and the disappearance of **5**.

Decomposition of [(tpfc)Mn^{V}(NHTs)]$^{+}$ (4): Detection of TsNH$_2$ by NMR Spectroscopy. A 2.0 mM solution of (tpfc)Mn^{V}NTs (**2**) was generated by combining 1.0 mg (1.2 μmol) of (tpfc)Mn (**1**) with 0.5 mg (1.0 μmol) of 2-(*t*-butylsulfonyl)(*p*-toluenesulfonyliminoiodo)-benzene in 0.50 mL of C_6D_6. A 0.10 M solution (10 μL) of CF_3COOH (1.0 μmol) in C_6D_6 was added. $TsNH_2$ was detected by ^{1}H NMR (δ = 4.74, s, 2H) and quantified by integration against ethyl acetate internal standard from **1**·$(EtOAc)_2$ (δ = 1.88, s, 3H, CH_3).

Acknowledgment. This work was supported by a grant from the National Science Foundation (Grant No. CHE-0502391).

Supporting Information Available: Kinetics plots of k_ψ versus concentration of substrate, EPR spectra of product organic radicals, data on determination of activation parameters, isokinetic plot, mass spectra for **4** and **5**, and absorption spectra for reaction of **2** with phenols. This material is available free of charge via the Internet at http://pubs.acs.org.

JA073027S